IOP PUBLISHING NANOTECHNOLOGY
Nanotechnology **18** (2007) 135708 (8pp) doi:10.1088/0957-4484/18/13/135708

Mechanical elasticity of vapour–liquid–solid grown GaN nanowires

Yunxia Chen[1], Ian Stevenson[2], Rebecca Pouy[2], Lidong Wang[2], David N McIlroy[2], Tyler Pounds[3], M Grant Norton[3] and D Eric Aston[1,4]

[1] Department of Chemical Engineering, University of Idaho, PO Box 441021, Moscow, ID 83844-1021, USA
[2] Department of Physics, University of Idaho, PO Box 440903, Moscow, ID 83844-0903, USA
[3] School of Mechanical and Materials Engineering, Washington State University, Pullman, WA 99164, USA

E-mail: aston@uidaho.edu

Received 6 November 2006, in final form 19 January 2007
Published 28 February 2007
Online at stacks.iop.org/Nano/18/135708

Abstract
Mechanical elasticity of hexagonal wurtzite GaN nanowires with hexagonal cross sections grown through a vapour–liquid–solid (VLS) method was investigated using a three-point bending method with a digital-pulsed force mode (DPFM) atomic force microscope (AFM). In a diameter range of 57–135 nm, bending deflection and effective stiffness, or spring constant, profiles were recorded over the entire length of end-supported GaN nanowires and compared to the classic elastic beam models. Profiles reveal that the bending behaviour of the smallest nanowire (57.0 nm in diameter) is as a fixed beam, while larger nanowires (89.3–135.0 nm in diameter) all show simple-beam boundary conditions. Diameter dependence on the stiffness and elastic modulus are observed for these GaN nanowires. The GaN nanowire of 57.0 nm diameter displays the lowest stiffness (0.98 N m^{-1}) and the highest elastic modulus (400 $\pm$ 15 GPa). But with increasing diameter, elastic modulus decreases, while stiffness increases. Elastic moduli for most tested nanowires range from 218 to 317 GPa, which approaches or meets the literature values for bulk single crystal and GaN nanowires with triangular cross sections from other investigators. The present results together with further tests on plastic and fracture processes will provide fundamental information for the development of GaN nanowire devices.

1. Introduction

Investigation of the mechanical properties of nanowires is essential and of significant importance to determine the material strength for practical implementation as electronic or optical interconnects, as components in microelectromechanics, and as active or passive parts in nanosensors [1–8]. Mechanical failure of those interconnects or building blocks may lead to malfunction or even fatal failure of the entire device. Mechanical reliability, to some extent, will determine the long-term stability and performance for many of the nanodevices currently being designed and fabricated. When nanowire properties have been adequately explored and understood, their incorporation into solutions of practical problems will become evident more quickly and feasible for active and concerted pursuit.

Since GaN was synthesized in 1932 [9], large quantities of data have established GaN as an important semiconductor material with wide bandgap (3.4 eV), possessing high thermal stability, chemical inertness and hardness. Its properties make it a suitable material for high-power, high-temperature, high-voltage and high-frequency electronic or optoelectronic device applications [10, 11]. Research interest in GaN nanowires has increased significantly in recent years because for sufficiently thin shapes such as nanowires, quantum confinement effects are expected to lead to novel or enhanced physical properties of potential use in future nanotechnology.

[4] Author to whom any correspondence should be addressed.

GaN nanowires have been reported in numerous works to show promise as elemental building blocks for photonic, electronic and optoelectronic nanodevices including logic gates, field-effect transistors (FETs), light-emitting diodes (LEDs), subwavelength photonics components and so-called 'nanolasers' [12–17]. For integration into true nanodevices, controllable assembly and precise location of fabricated nanowires must be accomplished in device architectures. A better understanding of mechanical behaviour is just one of many aspects that require detailed study.

To date, the mechanical properties of bulk GaN (or films) have been studied by various techniques, such as Brillouin scattering, resonance ultrasound and nanoindentation [18–21]. Classical molecular dynamics has been adopted to investigate theoretically the mechanical properties of GaN nanotubes under tension and fatigue [22, 23]. The related studies revealed that mechanical properties of GaN are related to the preparation, microstructure, size and the measurement technique in use. Electromechanical resonance analysis in a transmission electron microscope (TEM) was used previously to infer the Young's modulus (E) and quality factor of GaN nanowires [24]. The modulus obtained for an 84 nm nanowire was close to the theoretical bulk value; but the inferred values of E decreased gradually for smaller diameters, which is difficult to resolve against the present understanding of mechanics and materials at the nanoscale.

Several methods have been proposed to investigate the mechanical properties of nanowires. Among them, bending tests using atomic force microscopy (AFM) in different modes is most common, such as contact mode [2, 7, 8, 25, 26], lateral force mode [27, 28] and digital pulsed force mode (DPFM) [29, 30]. The force–distance behaviour measured with AFM is interpreted based on classic beam model theory to measure stiffness and strength of nanowires, usually only for isolated midpoint measurements. This approach is valid when the nanowires follow linear elastic theory of isotropic materials and have high length-to-thickness ratios [3]. Compared to other AFM operations, DPFM combines the advantages of imaging and simultaneously performing three-point bending tests at every point imaged along the suspended nanowire [29, 30], not just single-position measurements as reported elsewhere [2, 7, 8, 25, 27, 28]. This technique provides enough data to resolve the uncertainty of positioning the AFM tip right at the midpoint and to investigate the validity of boundary condition assumptions.

In this study, we applied DPFM AFM to the study of the mechanical elasticity of vapour–liquid–solid (VLS) [31] grown GaN nanowires with diameters in the range of 57–135 nm. The bending deflection and effective bending stiffness profiles were recorded over the entire length of end-supported GaN nanowires. Elastic moduli (E) for these nanowires were computed and compared on the basis of classic mechanics models. The findings for elasticity and boundary condition behaviour were investigated and are discussed in detail.

2. Experimental details

2.1. Nanowire growth and characterization

GaN nanowires were synthesized using an iron catalyst (60 nm) deposited on silicon substrates through direct reaction of Ga and ammonia (NH_3) at 900 °C and atmospheric pressure via a VLS mechanism with a similar procedure as that published elsewhere [32]. The reaction duration was 30 min and the flow rate for NH_3 was in the range of 5–10 ml min^{-1}. The produced GaN nanowires by this method have diameters in the range of 30–150 nm (mostly ∼85–140 nm) and lengths up to several hundred micrometres (figure 1(a)) as determined by field emission scanning electron microscopy (FE-SEM, SUPRA 35 VP, Zeiss). A transmission electron microscope (TEM, Philips CM200) 200 kV image shows the hexagonal cross section of a single GaN nanowire (figure 1(b)). The corresponding electron-diffraction pattern indicates that the nanowire is a single-crystalline hexagonal wurtzite structure with epitaxial growth orientation parallel to [0001]. The diffraction peaks (figure 1(c)) recorded with a Siemens D5000

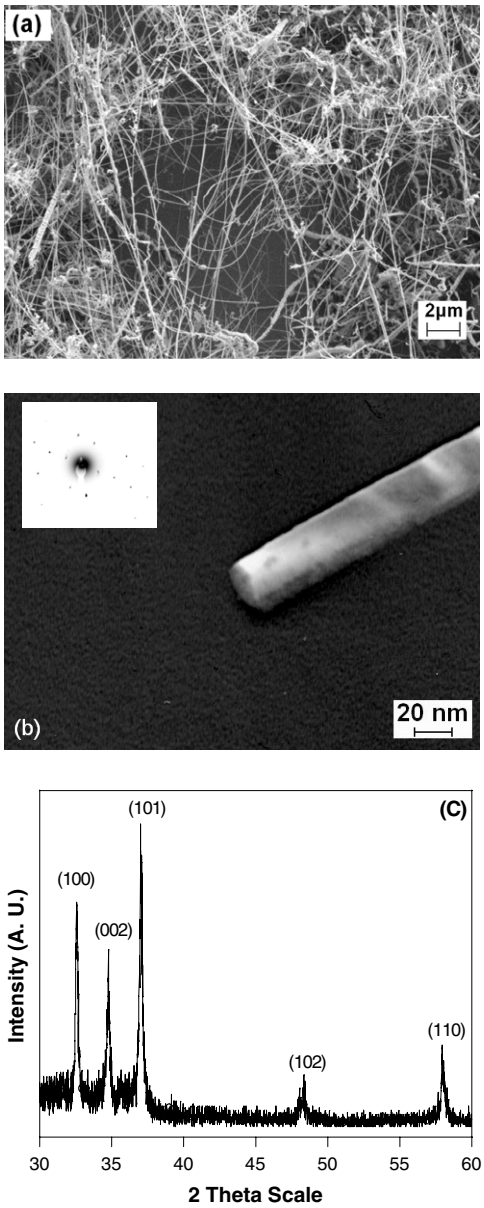

Figure 1. SEM image (a), dark-field TEM image and corresponding electron-diffraction pattern (b) and XRD pattern (c) of the synthesized GaN nanowires.

X-ray diffractometer (XRD), occurring at 32.5°, 34.7°, 36.6°, 48.3° and 58.1°, are indexed to (100), (002), (101), (102) and (110) facets and confirm that these GaN nanowires have the hexagonal wurtzite crystal structure (JCPDS File 02-1078), consistent with TEM results; micropowder XRD analysis also confirms the single-crystalline phase.

2.2. AFM sample preparation

Rectangular silicon gratings (TGZ-03, MikroMasch) for AFM scanner calibrations were used as the microchannel supports for three-point bending tests. The grating used in this study has pitch widths of 3 μm and depths of 0.5 μm. Before transferring nanowires, the grating was spin-coated with a ∼10–20 nm layer of poly(perfluoro N-octyl methacrylate) (PFOM) thermopolymer synthesized from its monomer. The PFOM thin film was prepared as follows: 20 μl perfluorocarbon C7F16 (PF5070, 3M Corp.) solution was dropped with a micropipette onto the centre of the stationary silicon grating (5×5 mm^2), then spun at 4500 rpm for 60 s. The grating was then placed on a hot plate and heated up to 120 °C to soften the thin film. Nanowires grown on a separate silicon substrate were subsequently transferred to the hot grating by direct physical contact. After cooling, the hardened polymer thin film helps to glue the otherwise fairly non-sticking system. As a result, nanowires are randomly suspended across microchannels, many with both ends conveniently supported for a three-point bend test, as shown in figure 2.

Because the nanowires were not perfectly aligned perpendicular to the trenches, the gauge length is measured in each case from AFM and SEM images by assuming no sagging or residual stress. Before AFM scanning, nanowires were first located and selected on the grating with high-resolution dark-field microscopy (BX51 microscope, Olympus), and the same nanowires were relocated and analysed by FE-SEM for determining diameters and checking for any possible damage after bending tests. We found that nanowires spring back to their original position and no obvious indentation or fracture occurred, indicating their complete elasticity. The nanowire diameter determined from the transverse width measured with SEM is more precise than that from the height measured with AFM, because part of the nanowire may lay buried in the polymer thin-film.

The three-point bend tests of GaN nanowires were made by scanning along the nanowire length using an AFM tip with DPFM operation (WITec, Germany). The normal cantilever force constants, AFM scanner and photodetector sensitivities, and DPFM modulation factor were calibrated in order to conduct precise quantitative analysis of mechanical results [29]. The cantilevers (spring constant of ∼3 N m^{-1}) from Budget Sensors were used in our research, and carefully calibrated using the method of Sader *et al* [33]. The deflection voltage–time curves then can be converted to real force–deflection curves for each pixel of interest on the nanowire. The linearity and coincidence of the approach and retraction portions of the force–deflection curves proved that the nanowire bending was linear and elastic, which is consistent with the SEM results of nanowires after bending tests. Imaging at large and small scan ranges could be repeated without movement of the nanowires.

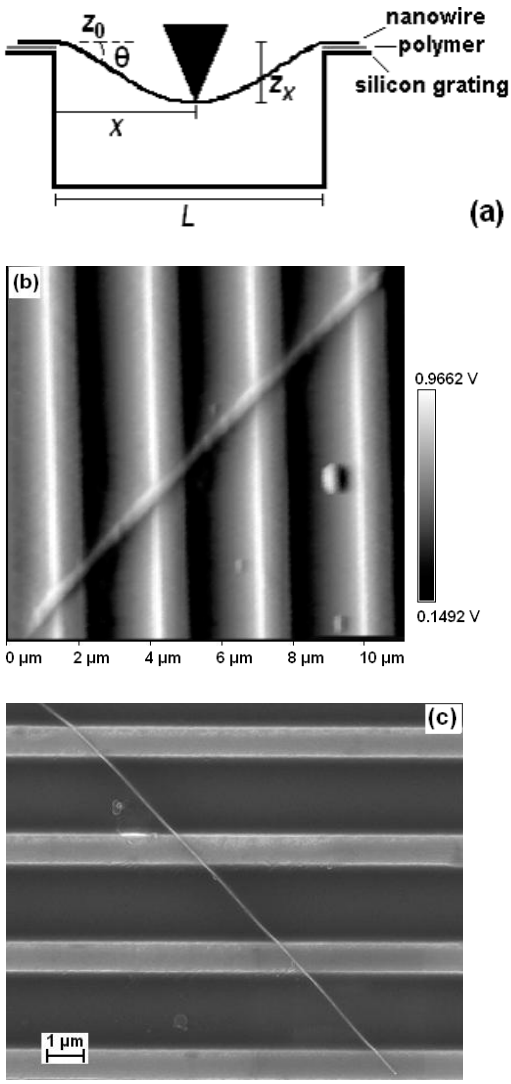

Figure 2. (a) Schematic diagram of the nanowire bending test with an AFM tip; (b), (c) DPFM maximum force image and SEM image of an individual GaN nanowire (57.0 nm) aligned across a silicon microchannel.

The actual bent deflection (z_x) was calculated by using [34]

$$z_x = (z - z_0) - \Delta z_c, \tag{1}$$

where z_0 and z are the AFM position at initial and measurement points, x, and Δz_c is the cantilever deflection. To compensate for possible indentation of the polymer coating or substrate, the deflection measured on the nanowire segment supported by the silicon substrate (z_0) was subtracted from the deflections of the suspended section [7]. Then, based on the applied load, F, and corresponding deflection, the effective bending stiffness of the nanowire is from Hooke's law

$$k = F/z_x. \tag{2}$$

The DPFM data acquired along the centreline of the nanowire are analysed to obtain bending deflection and effective stiffness profiles of nanowires based on two classic models for elastic deflections of a beam with circular cross section: with fixed

Table 1. Applied force (point load) on individual GaN nanowires and corresponding maximum deflection, bending angle and minimum effective stiffness.

No	Diameter (nm)	Length (nm)	Diameter to length ratio	Force (nN) Range	Force (nN) Average	Maximum deflection (nm)	Bending angle (deg)	Minimum stiffness (N m^{-1})
1	57.0	3054	53	98.8–122.7	107.8	109.1	4.1	0.98
2	89.3	2398	27	88.3–136.7	112.3	53.7	2.6	2.10
3	94.5	2427	26	38.7–72.1	53.5	31.6	1.5	2.13
4	97.8	2465	25	101.1–127.7	111.1	44.0	2.0	2.56
5	105.0	2611	25	123.4–166.4	139.4	43.9	1.9	3.23
6	109.7	2558	23	174.7–203.8	189.5	47.8	2.1	3.95
7	110.0	2220	20	263.8–274.6	269.5	55.5	2.9	4.83
8	111.0	2048	18	101.7–113.9	108.7	16.8	0.9	6.49
9	135.0	1794	13	273.8–300.5	283.9	16.0	1.0	17.32

or clamped ends (fixed model) and with simply supported ends (simple model). Two ends of the nanowires are clamped against bending moments in the fixed model, while the simple model allows free motion. The relationships between elastic modulus E and deflection z_x with a suspended (gauge) length of L at a certain tip position x subjected to a load F are given by [35–37]

$$\text{Fixed model:} \qquad EIz_x = -\frac{F}{3L^3} \cdot x^3 \cdot (L-x)^3 \qquad (3)$$

$$\text{Simple model:} \qquad EIz_x = -\frac{F}{3L} \cdot x^2 \cdot (L-x)^2 \qquad (4)$$

where I is the cross-sectional moment of inertia; $I = 5\sqrt{3}r^4/16$ for a solid, regular hexagon with a side length of r. The best fits to experimental deflection profiles were determined by shape comparison of classic models against the data using an average value for E as the fitted parameter. As shown later, the tested nanowires show maximum deflection at the middle with nearly symmetric profiles. Consequently, the mixed beam model (one end is simply supported and the other is fixed) used in our previous studies [30] was not relevant.

3. Results and discussion

Table 1 lists the maximum point force on the GaN nanowires applied at each pixel, the corresponding maximum deflection at the midpoint and bending angles near the edges for a midpoint deflection. All tested GaN nanowires display small bending angles ($<4.1°$) under applied force, and they have high length-to-diameter ratios ($L/D > 13$, mostly > 20), which make classic elastic beam theories valid for quantitative comparison in our case [35]. As expected, higher applied loads or smaller diameters gave rise to larger maximum deflections near the midpoint. For example, for comparable diameters of nanowires #6–8, nanowire #8 deflected 16.8 nm under a set-point load of ~110 nN, less than half the loading force of nanowire #7. The maximum deflection of nanowire #7 under ~270 nN load was 55.5 nm. A comparison of nanowire deflections under similar loading conditions (#1, #2, #4, #8) demonstrates the consistent and expected trend of decreasing midpoint deflection with increasing nanowire diameter.

Knowing the boundary conditions for bending profiles is extremely important for measuring the elastic modulus of nanowires accurately. A fixed-beam boundary shows a shallow slope in the deflection profile near the ends and has more curvature throughout the profile, while a simple-beam boundary gives a steeper slope at the ends, and the profile is more parabolic in shape rather than the subtle S-curve of the fixed beam. Profiles for mixed boundaries (one simply supported and one fixed) would show intermediate values of deformation and be asymmetric about the midpoint. Bending profiles of typical nanowires have been plotted as a function of relative tip position x/L, *as* shown in figure 3, to illustrate the experimental boundary conditions observed for GaN nanowires. The maxima in deflection at the middle and profile symmetry indicate comparable boundary conditions at each supported end. Accordingly, in this paper, only fixed and simple-beam models were needed to describe the bending tests. Theoretical profiles for fixed and simple beams are also shown in figure 3. The bending profile for a 57.0 nm nanowire shows a smoother transition in slope from the edge toward the midpoint, which is the main feature of fixed ends. All other tested nanowires, with diameters ranging from 89.3 to 135.0 nm, show sharper and steeper sloping for edge deflections, best fitted by the simple-beam boundary condition. All experimental deflection profiles exhibit a reasonable fit, though not perfect, with theoretical values from fixed or simple-beam models.

These findings are similar to previous DPFM data for silver nanowires but different from earlier experiments on polymer nanowires (silver and polymer nanowires did not require a polymer adhesion layer) [29, 30]. The deflection profiles of polymer nanowires were best fitted with a fixed-beam model even though they were quite large (170–200 nm). Silver nanowires showed fixed-end behaviour for smaller diameters under low loading conditions and resulted in simple supports for larger diameters, which consequently required high loading for similar deflections. Large silver nanowires under low applied force exhibited intermediate conditions, probably due to transitions from fixed to simple ends with increasing stress. Higher work of adhesion with the substrate was suspected for small nanowires due to increased capillary effects, or meniscus forces [30]. However, under relatively large applied force, the work of adhesion is not always sufficient to resist the resultant stresses.

Compared to silver, GaN nanowires show relatively weak adhesion to the substrate, demonstrated from initial AFM images on the silicon test gratings without a polymer adhesion layer. Though the polymer thin film improved adhesion, it was still insufficient in most cases for larger nanowires. Aside from nanowire size and experimental loading, this suggests that the

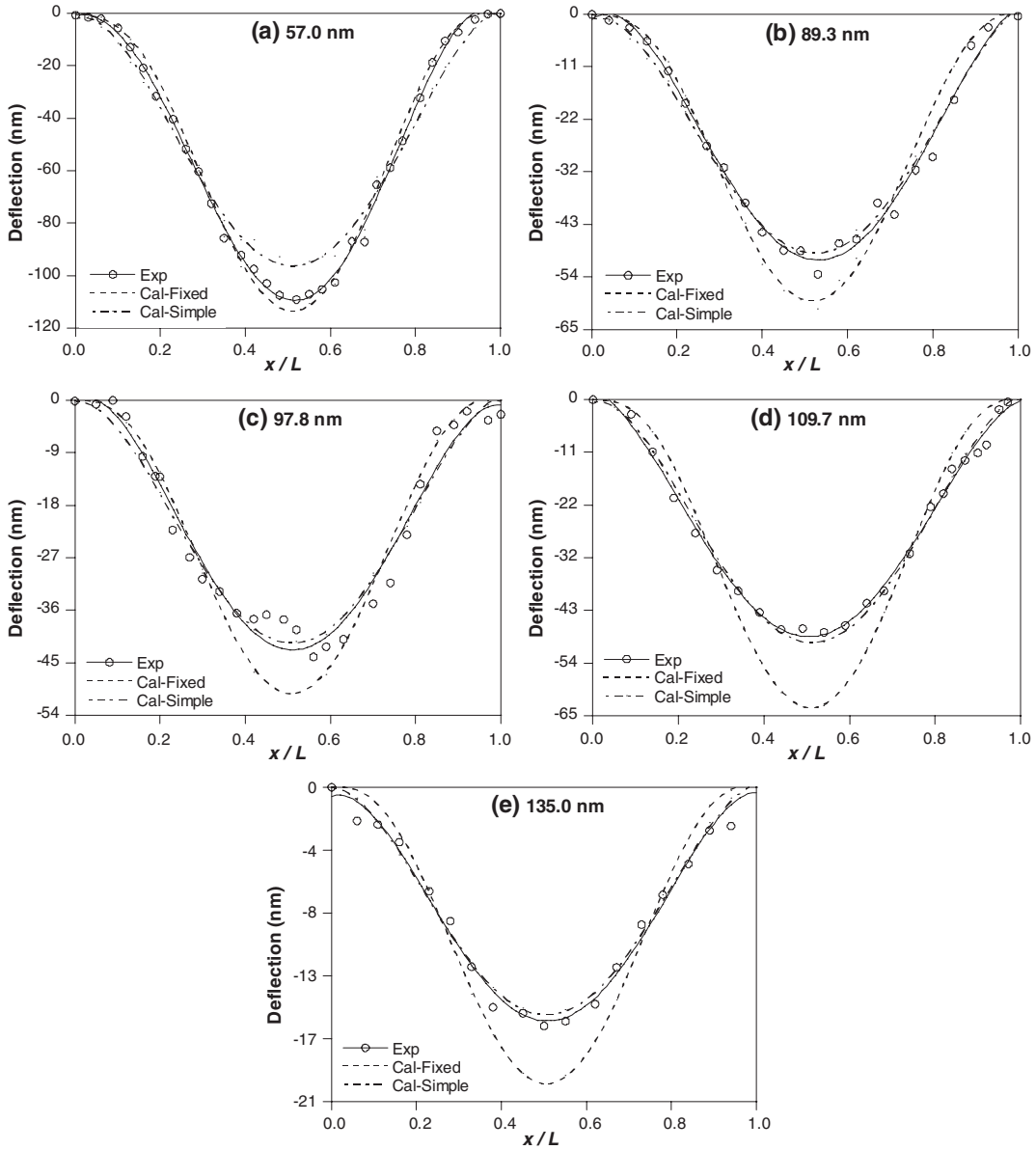

Figure 3. Comparison of experimental and model deflections for tested GaN nanowires.

intrinsic surface energy of GaN nanowires is quite low, as is well known of boron nitride. (Contact angle measurements with the water on substrates of random GaN nanowire coatings also exhibit complete nonwetting.) In the future, we will be investigating the adhesion between nanowire and substrate in order to obtain a comprehensive understanding of boundary conditions in bending tests.

Figure 4 displays effective bending stiffness profiles of selected GaN nanowires as a function of relative tip position x/L compared to fixed and simple models. As expected, effective bending stiffness of GaN nanowires increases from the midpoint to the edges, and it is inclined to infinity at the ends. As listed in table 1, the minimum stiffness (at the midpoint) increases regularly from 0.98 to 17.32 N m^{-1} as nanowire diameters increase from 57.0 to 135.0 nm. Stiffness profiles of GaN nanowires (except for ⌀57.0 nm case, which is fixed) exhibit a reasonable fit with theoretical stiffness as a simple beam. Deviations near the edges are due to increased experimental sensitivity of the three-point bending design and magnification of errors since the actual boundary conditions are not perfect.

After confirming the boundary conditions, GaN nanowire elastic moduli were computed using the appropriate model. Figure 5 shows elastic modulus for GaN nanowires versus diameters; decreasing from 400.1 ± 14.9 GPa (standard deviation errors) to 195.6 ± 19.7 GPa as diameter increases from 57 to 135 nm. The value of 400 GPa for 57 nm nanowire is from the fixed-beam model, while the simple-beam model was found to be valid for the 89.3–135.0 nm range. Moduli trends similar to our results were reported for many other nanowires, such as ZnO, SiC and TiO_2. The elastic modulus for ZnO nanowires with diameters smaller than 120 nm increases dramatically with decreasing diameters and is significantly higher than larger nanowires or bulk

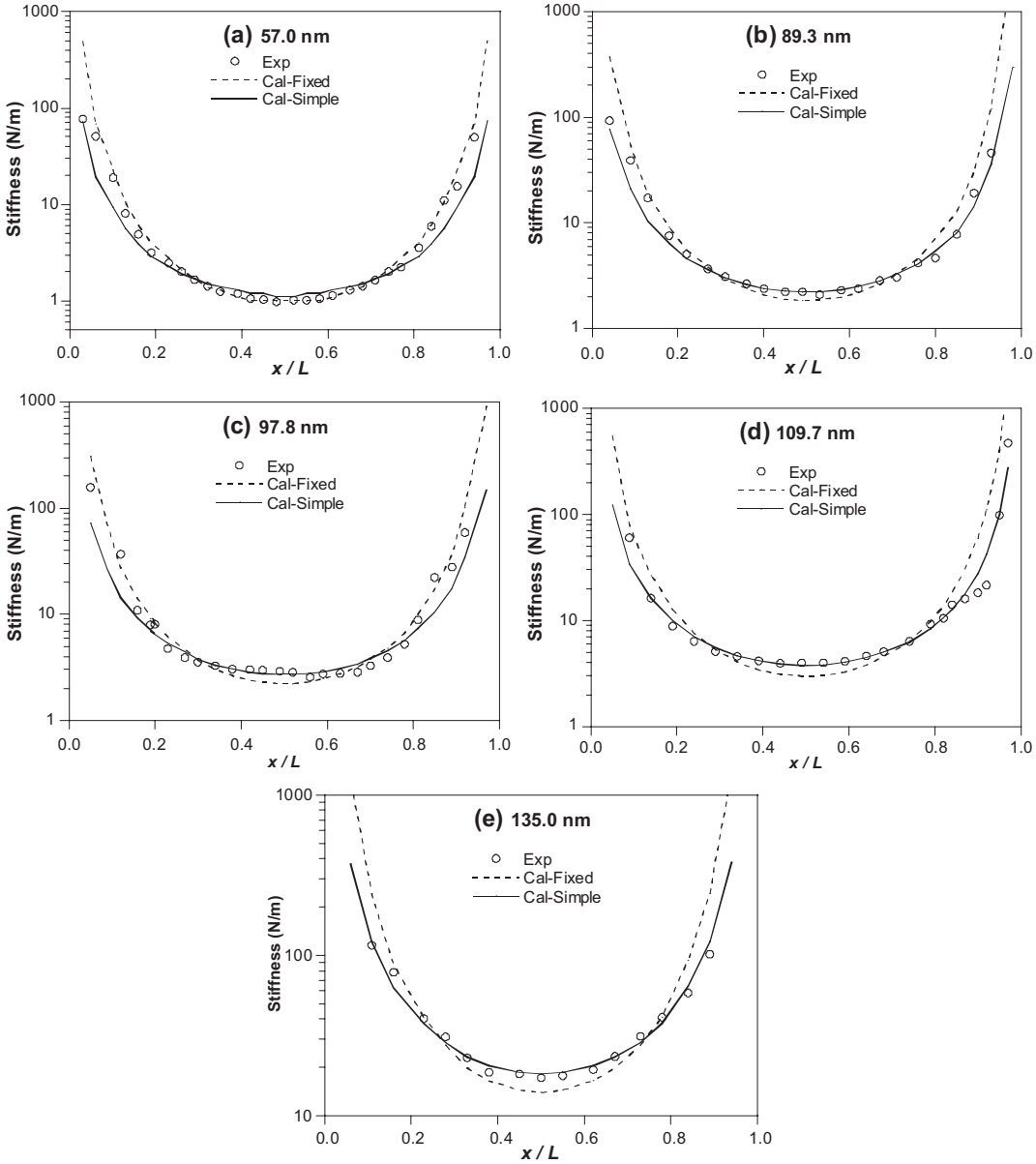

Figure 4. Comparison of experimental and model effective stiffness for tested GaN nanowires.

ZnO [38]. SiC nanorods were reported to approach the theoretical value for E when the diameter was reduced to ∼20 nm [39]. Generally, physical properties such as elastic modulus are believed to be directly related to the material structural perfection [40]. The elastic stiffening for smaller nanowires can be explained by the lower probability of finding a defect in smaller volumes [38–40]. However, these findings are different from the results of silver and triangular GaN nanowires.

In our previous work, no obvious size dependence on E was observed for silver nanowires [30]. The opposite trend was observed in E for triangular GaN nanowires within the diameter range of 36–84 nm [24]. The authors suggested this converse behaviour was due to the increase of surface-to-volume ratio (S/V) with decreasing d. They believed the atomic coordination and cohesion near the surface were 'poor' relative to bulk, and the increasing dominance of the surface would decrease the rigidity of the structure [41]. Furthermore, nanowire shape and, microstructure are also determinate contributions to the difference in observed moduli trends: the GaN nanowires we produced have a hexagonal cross section grown along the [0001] direction (figure 1(b)), while those of [24] have a triangular cross-sectional shape grown along the [120] direction.

For most nanowires with diameters of 89–110 nm, the simple-beam model gave $E = 218.1$–316.9 GPa, which approaches or meets the literature values of ∼295 GPa for bulk single crystal [19–21, 42]. Literature values for GaN nanowires with triangular cross sections were similar: 227–305 GPa for 36–84 nm diameter [24]. But for the smallest nanowire with diameter of 57.0 nm, E is as high as 400.1 ± 14.9 GPa from the fixed-beam model, which far exceeds the literature values. This

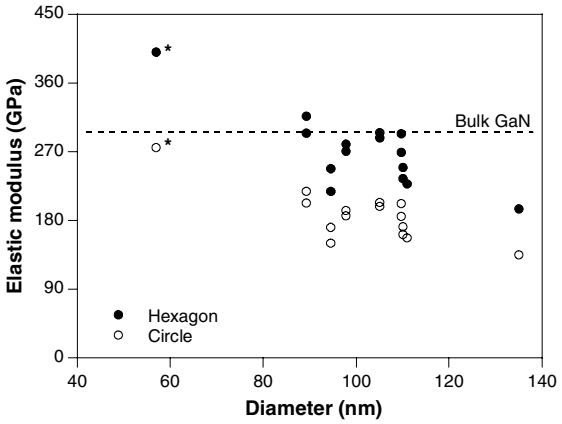

Figure 5. Elastic moduli for tested GaN nanowires versus nanowire diameters from the simple-beam model (*fixed-beam model).

may be due to variations in nanowire shape. Though the TEM image reveals a nearly hexagonal cross section for the GaN nanowire, it is not perfect. In fact, it is more like a 'circular' hexagon. For cross sections of regular circular and hexagonal shape, their inertial moments are as follows: $I_c = \pi r^4/4$ for a solid circular area with a radius of r and $I_h = 5\sqrt{3}r^4/16$ for solid regular hexagon with a side length of r, respectively. For a given nanowire deflection, the calculated E using a hexagonal cross section would be 45% larger than that with a circular cross section for the same observable width (figure 5). For relatively small nanowires, this becomes significant due to the fourth-order dependence in I on diameter.

With the boundary condition issue essentially solved, the practical uncertainty of diameter size and shape are the most significant sources of persisting error in nanomechanics. This error cannot be precisely determined because the exact shape of a specific nanowire is not available for confirmation. In addition, compared to those literature values, E for some tested GaN nanowires is low. Microstructure differences may contribute to this discrepancy. Via FE-SEM and TEM images, we have observed that some nanowires are not uniform in diameter or smooth on the surface. These microstructural irregularities may weaken the nanowire, as well as complicating comparison with the standard beam model assuming a uniform cross section. Obvious elastic weakening for nanowires or nanobelts was also observed in ZnO [6], lead zirconate titanate (PZT) [8] and ZnS [42, 43] compared to bulk materials. Elastic modulus of ZnO nanowires is even smaller (80%) than that of the bulk [6].

The theoretical propagation of errors is due primarily to uncertainty in

(i) nanowire diameter, and to a lesser degree, gauge length,
(ii) the use of a polymer adhesion layer,
(iii) boundary conditions,
(iv) shear deflection and indentation, and
(v) AFM scanner and detector calibrations, and cantilever stiffness.

Among them, the uncertainty in nanowire diameter is responsible for the greatest magnitude in total uncertainty of calculated E values. As discussed earlier, the classic elastic beam model is valid only under the assumption of a homogeneous beam, that is, constant and uniform E and I. Very slight variations in diameter are significant because of the fourth-order dependence in I of equations (3) and (4), resulting in an experimental error of ∼10%. The error due to length is insignificant at ∼0.3%. The polymer coating helped adhere to the nanowire but makes an absolute determination of nanowire deflection theoretically impossible, since there is no method to measure the compressibility of that layer independently for the three-point bending experiment with precision. Instead, the best solution is to subtract the indentation as measured on the supported end, which is currently the standard approach in the literature [7]. Due to high length-to-diameter ratio of tested nanowires and relatively low applied loads, shear and indentation deformation are insignificant. Even under the maximum experimental force (300 nN), both shear deformation and indentation are estimated as less than 0.3 nm (estimated with a spherical AFM tip), which gives an experimental error of ∼1.7%.

The plastic and fracture process of these nanowires and their aging were not evaluated in the current study and cannot be deduced directly from consideration of mechanical elasticity. Extended experiments with increased applied loads, bending frequency and repetitions on GaN nanowire with both ends fixed can be pursued to advance the investigation of mechanical properties of nanowires and size–property relationships. Those findings will provide more detailed information for development of GaN nanowire devices. Increased failure strength is expected with decreased nanowire physical dimensions, due to the lower concentration of critically sized defects [44].

4. Conclusions

Mechanical elasticity of hexagonal wurtzite GaN nanowires with hexagonal cross sections grown via a VLS method have been investigated with advanced digital capabilities of AFM. Diameter dependence on the stiffness and elastic modulus is observed for these GaN nanowires (57.0–135.0 nm ⌀). With increasing diameter, elastic modulus decreases while stiffness increases. The bending behaviour of the nanowire with the smallest diameter (57 nm) reveals fixed-beam boundary conditions, while larger nanowires (89.3–135.0 nm) appear as simple beams that do not resist bending moments at the supported ends. The GaN nanowire of 57.0 nm diameter displays the lowest stiffness, or spring constant (0.98 N nm^{-1}), and the highest elastic modulus (400.1 ± 14.9 GPa). Elastic moduli for most tested nanowires range from 218.1 to 316.9 GPa, approaching or exceeding literature values for bulk single crystal and GaN nanowires with triangular cross sections, reported by others. These moduli are based on the assumption that all tested nanowires were of a hexagonal wurtzite structure with hexagonal cross sections, which is supported by complementary analytical techniques but cannot be known for certain of every nanowire. This uncertainty must be resolved before determining direct diameter-dependence effects on elasticity for GaN. With the details of the boundary condition well documented and understood, the practical uncertainty of variations in diameter size and shape for each individual nanowire are the most significant sources

of persisting error in nanomechanics. The coauthors are designing a combined AFM and spectroscopic experiment using *in situ* scanning Raman techniques to investigate the possibility of structural confirmation with adequate spatial resolution to identify each nanowire.

Acknowledgments

The authors gratefully acknowledge the support of the National Science Foundation (EPS-0132626, EPS-0447689) and the W M Keck Foundation. We thank Franklin Bailey, Brendan Twamley and Tom Williams at the University of Idaho for their SEM and XRD analyses. We also thank Glen Dunham at Pacific Northwest National Laboratory for supplying the polymer solution.

References

[1] Heidelberg A, Ngo L T, Wu B, Phillips M A, Sharma S, Kamins T I, Sader J E and Boland J J 2006 *Nano Lett.* **6** 1101
[2] Ni H, Li X D and Gao H S 2006 *Appl. Phys. Lett.* **88** 043108
[3] Withers J R and Aston D E 2006 *Adv. Colloid Sci.* **120** 54
[4] Cuenot S, Demoustier-Champagne S and Nysten B 2000 *Phys. Rev. Lett.* **85** 1690
[5] Li X D, Nardi P, Baek C-W, Kim J-M and Kim Y-K 2005 *J. Micromech. Microeng.* **15** 551
[6] Song J H, Wang X D, Riedo E and Wang Z L 2005 *Nano Lett.* **5** 1954
[7] Humar M, Arcon D, Umek P, Škarabot M, Muševič I and Bregar G 2006 *Nanotechnology* **17** 3869
[8] Xu S, Shi Y and Kim S 2006 *Nanotechnology* **17** 4497
[9] Johnson W C, Parsons J B and Crew M C 1932 *J. Phys. Chem.* **36** 2561
[10] Strite S and Morkoç H 1992 *J. Vac. Sci. Technol.* B **10** 1237
[11] Morkoç H 1999 *Nitride Semiconductors and Devices* (Heidelberg: Springer)
[12] Huang Y, Duan X, Cui Y, Lauhon L J, Kim K H and Lieber C M 2001 *Science* **294** 1313
[13] Huang Y, Duan X F, Cui Y and Lieber C M 2002 *Nano Lett.* **2** 101
[14] Zhong Z H, Qian F, Wang D L and Lieber C M 2003 *Nano Lett.* **3** 343
[15] Johnson J C, Choi H-J, Knutsen K P, Schaller R D, Yang P and Saykally R J 2002 *Nat. Mater.* **1** 106
[16] Stern E *et al* 2005 *Nanotechnology* **16** 2941
[17] Pauzauskie P J, Sirbuly D J and Yang P D 2006 *Phys. Rev. Lett.* **96** 143903
[18] Polian A, Grimsditch M and Grzegory I 1996 *J. Appl. Phys.* **79** 3343
[19] Drory M D, Ager J W III, Suski T, Grzegory I and Porowski S 1996 *Appl. Phys. Lett.* **69** 4044
[20] Schwarz R B, Khachaturan K and Weber E R 1997 *Appl. Phys. Lett.* **70** 1122
[21] Nowak R, Pessa M, Suganuma M, Leszcynski M, Grzegory I, Porowski S and Yoshida F 1999 *Appl. Phys. Lett.* **75** 2070
[22] Jeng Y R, Tsai P C and Fang T H 2004 *Nanotechnology* **15** 1737
[23] Jeng Y R, Tsai P C and Fang T H 2005 *J. Nanosci. Nanotechnol.* **8** 191
[24] Nam C Y, Jaroenapibal P, Tham D, Luzzi D E, Evoy S and Fisher J E 2006 *Nano Lett.* **6** 153
[25] Bellan L M, Kameoka J and Craighhead H G 2005 *Nanotechnology* **16** 1095
[26] San Paulo A, Bokor J, Howe R T, He R, Yang P, Gao D, Carraro C and Maboudian R 2005 *Appl. Phys. Lett.* **87** 053111
[27] Wu B, Heidelberg A, Boland J J, Sader J E, Sun X M and Li Y D 2006 *Nano Lett.* **6** 468
[28] Wu B, Heidelberg A and Boland J J 2005 *Nat. Mater.* **4** 525
[29] Shanmugham S, Jeong J, Alkhateeb A and Aston D E 2005 *Langmiur* **21** 10214
[30] Chen Y X, Dorgan B L Jr, McIlroy D N and Aston D E 2006 *J. Appl. Phys.* **100** 104301
[31] Wagner R S and Ellis W C 1964 *Appl. Phys. Lett.* **4** 89
[32] Chen C C, Yeh C C, Chen C H, Yu M Y, Liu H L, Wu J J, Chen K H, Chen L C, Peng J Y and Chen Y F 2001 *J. Am. Chem. Soc.* **123** 2791
[33] Sader J E 2005 *Atomic Force Microscope Cantilevers (Calibration Method of Sader)* Department of Mathematics and Statistics, University of Melbourne Website
[34] Tombler T W, Zhou C W, Alexseyev L, Kong J, Dai H J, Liu L, Jayanthi C S, Tang M J and Wu SY 2000 *Nature* **405** 769
[35] Gere J M and Timoshenko S P 1997 *Mechanics of Materials* (Boston, MA: PWS Publishing)
[36] Pikey W D 1994 *Formulas for Stress, Strain, and Structural Matrices* (New York: Wiley)
[37] Roark R J and Young W C 1975 *Formulas for Stress and Strain* (New York: McGraw-Hill)
[38] Xiong Q, Duarte N, Tadigadapa S and Eklund P C 2006 *Nano Lett.* **6** 1904
[39] Wong E W, Sheehan P E and Lieber C M 1997 *Science* **277** 1971
[40] Cuenot S, Demoustier-Champagne S and Nysten B 2000 *Phys. Rev. Lett.* **85** 1690
[41] Schmid M, Hofer W, Varga P, Stoltze P, Jacobsen K W and Nørskov J K 1995 *Phys. Rev.* B **51** 10937
[42] Chen C Q, Shi Y, Zhang Y S, Zhu J and Yan Y J 2006 *Phys. Rev. Lett.* **96** 075505
[43] Li X, Wang X, Xiong Q and Eklund P C 2005 *Nano Lett.* **5** 1982
[44] Silva E C C M, Tong L, Yip S and Vliet K J V 2006 *Small* **2** 239